

Theory for the coupling between longitudinal phonons and intrinsic Josephson oscillations in layered superconductors

Ch. Helm, Ch. Preis, Ch. Walter, and J. Keller
*Institut für Theoretische Physik, Universität Regensburg,
D-93040 Regensburg, Germany*
(October 16, 2019, submitted to PRB)

In this publication a microscopic theory for the coupling of intrinsic Josephson oscillations in layered superconductors with longitudinal *c*-axis-phonons is developed. It is shown that the influence of lattice vibrations on the *c*-axis transport can be fully described by introducing an effective longitudinal dielectric function $\epsilon_{\text{ph}}^L(\omega)$. Resonances in the *I*-*V*-characteristic appear at van Hove singularities of both acoustical and optical longitudinal phonon branches. This provides a natural explanation of the recently discovered subgap structures in the *I*-*V*-characteristic of highly anisotropic cuprate superconductors. The effect of the phonon dispersion on the damping of these resonances and the coupling of Josephson oscillations in different resistive junctions due to phonons are discussed in detail.

74.80Dm, 74.50+r, 74.25Kc, 74.25Jb

I. INTRODUCTION

The *c*-axis transport in the highly anisotropic cuprate superconductors $\text{Tl}_2\text{Ba}_2\text{Ca}_2\text{Cu}_3\text{O}_{10+\delta}$ (TBCCO) and $\text{Bi}_2\text{Sr}_2\text{CaCu}_2\text{O}_{8+\delta}$ (BSCCO) can well be described by a stack of Josephson junctions between the superconducting CuO_2 -multi-layers. This intrinsic Josephson effect can be seen in the multi-branch structure of the *I*-*V* characteristic. Here each branch corresponds to a well-defined number of junctions in the resistive, oscillating state.^{1,2} The intrinsic Josephson effect is observed also in the behaviour of the material in external magnetic fields and with microwave irradiation.^{1,2}

Recently subgap structures in the *I*-*V*-characteristic have been discovered as intrinsic properties of the material,^{3–5} which could be explained by the coupling between the intrinsic Josephson oscillations and phonons.^{6–8} This interaction is mediated by the oscillating electric field in the Josephson junction, which excites vibrations of charged ions in the material. In our previous investigations^{6,7} we used a simple model of a system of damped harmonic oscillators in order to describe the dynamics of oscillating ions in the barrier. We were able to derive an analytic expression for the dc-current density $j(V)$ as function of the dc-voltage V for one resistive junction

$$j(V) = j_{qp}(V) + \frac{j_c}{2} \frac{\omega_p^2}{\omega^2} \frac{\epsilon_2 + \frac{\sigma}{\omega\epsilon_0}}{\epsilon_1^2 + (\epsilon_2 + \frac{\sigma}{\omega\epsilon_0})^2}. \quad (1)$$

where the voltage V is related to the Josephson frequency ω by $V = \hbar\omega/(2e)$ and $\epsilon(\omega) = \epsilon_1(\omega) + i\epsilon_2(\omega)$ is the dielectric function of the oscillating ions. From this result it can be seen that the *I*-*V*-curve has a maximum at the frequency (voltage) where the real part ϵ_1 of the phonon-dielectric function vanishes, which corresponds to a longitudinal eigenfrequency of the phonon system.

With appropriate values for the Josephson plasma frequency ω_p , the quasiparticle conductivity σ , the critical current density j_c , and the frequencies, dampings and oscillator strengths of phonons in the dielectric function we were able to fit the experimental results for the subgap structures in the *I*-*V*-curves perfectly. In addition to this, the identification of the maxima of the structure with phonon frequencies provides a natural explanation, why the position of the resonances is completely independent of temperature, magnetic field and the geometry of the probe. The voltage positions of these resonances can also be related to structures in optical experiments,^{9,10} in particular to the reflectivity for oblique incidence.¹¹

Despite the clear evidence of the effect a general multi-band theory, in which the phonon parameters are specified microscopically, is still missing and shall be presented in the following. In particular, in Refs. 6,7 the phonon frequencies and the oscillator strengths in the dielectric function were not specified. The clarification of this point and the extension to a general lattice dynamical model including acoustical and optical branches and several resistive junctions will be the main purpose of the following investigation. It turns out that the basic structure of the result Eq. (1) will be the same as before with the phonon dielectric function replaced by a more general expression.

The excitation of phonons by Josephson oscillations in single Josephson junctions has been observed already a long time ago.¹² Also in the *I*-*V* curves of break-junctions of cuprate-superconductors¹³ structures due to phonons could be identified. The physical mechanism described here can also be applied to these cases but our formalism is particularly suited to treat stacks of Josephson junctions with phonons in the frequency range between the Josephson plasma frequency and the gap-frequency.

The paper is organized as follows: After a short derivation of the basic Josephson equations for a stack of junctions the electron-phonon interaction and its effect on the electronic transport perpendicular to the superconducting layers is derived microscopically. Special attention is paid to the correct choice of the driving electric field for conduction electrons and ions and the proper definition of

the phononic dielectric function. In particular we analyse the coupling strength for phonons of different branches and discuss the influence of the phonon dispersion on the subgap structures. By using a simple lattice-dynamical model we show that both acoustic and optical modes may couple to Josephson oscillations, i.g. the coupling of an acoustic mode at the boundary of the Brillouin zone may explain a structure at low dc-voltage,⁵ which could not be interpreted up to now.

The results are obtained both by numerical integration of the coupled equations of motion of phonons and Josephson oscillations and by approximate analytical calculations in the limit of large values of the McCumber parameter.

II. COUPLING BETWEEN PHONONS AND INTRINSIC JOSEPHSON OSCILLATIONS

We consider a system of N superconducting layers separated by insulating barrier material of thickness d forming a stack of Josephson junctions. We treat the superconducting layers as homogeneous metal sheets with a uniform electron distribution along the layers. In this paper we consider only the case of a uniform tunneling current with a constant bias-current and neglect magnetic field effects due to the current flow. In this case all quantities are constant along the layers.

The tunneling current density j_n from layer n to $n+1$ creates (two-dimensional) charge density fluctuations $\delta\rho_n$ on the layers related by the continuity equation

$$j_n(t) - j_{n-1}(t) = -\delta\dot{\rho}_n(t). \quad (2)$$

These charge fluctuations create electric fields $E_n^\rho(t)$ (in c-direction) in the barrier between layer n and $n+1$ which are constant inside each barrier and are related to the charge fluctuations by the Maxwell equation:

$$\delta\rho_n(t) = \epsilon_0 \left(E_n^\rho(t) - E_{n-1}^\rho(t) \right) \quad (3)$$

or

$$E_n^\rho(t) = \frac{1}{2\epsilon_0} \left(\sum_{n' \leq n} \delta\rho_{n'}(t) - \sum_{n' > n} \delta\rho_{n'}(t) \right). \quad (4)$$

Assuming that the current density j_n for the first and last barrier is fixed by the bias current density j , then with help of Eqs. (2,3) the tunneling current density j_n in all the other junctions is related to the bias current density j by

$$j = j_n(t) + \dot{D}_n(t). \quad (5)$$

Thereby in the last term the displacement current density $\dot{D}_n(t) := \epsilon_0 \dot{E}_n^\rho(t)$ has been introduced in order to relate the present results to the usual formulation of the RSJ model.

In the following we approximate the tunneling current by a superposition of a Josephson supercurrent density and a quasiparticle current density. Then we have for each junction:

$$j = j_c \sin \gamma_n(t) + j_{qp}(E_n(t)) + \dot{D}_n(t). \quad (6)$$

The Josephson current density $j_c \sin \gamma_n(t)$ depends on the gauge invariant phase difference $\gamma_n(t)$ between layers n and $n+1$ at positions z_n and z_{n+1} . It is related to the average total electric field in the barrier

$$E_n(t) := \frac{1}{d} \int_{z_n}^{z_{n+1}} E_z(z, t) dz \quad (7)$$

by the second Josephson equation

$$\hbar\dot{\gamma}_n(t) = 2eE_n(t)d. \quad (8)$$

Here possible small corrections to Eq. (8) for layered superconductors which are discussed in Refs. 14,15 are neglected. For the quasi-particle current density we will use in the following for simplicity an ohmic form $j_{qp} = \sigma E_n$ with a constant conductivity σ . The generalisation to more realistic forms⁷ is straight-forward.

The crucial point where the phonons come into play is the relation between the field $D_n = \epsilon_0 E_n^\rho$, which is created by the charge fluctuations on the superconducting layers alone, and the average electric field Eq. (7) $E_n = E_n^\rho + E_n^{\text{ion}}$ which contains also the averaged field E_n^{ion} created by the ionic displacements in the barrier. This will be discussed in detail below.

Before we do this let us summarise the most important parameters which characterise the Josephson system: The first one is the (bare) Josephson plasma frequency ω_p defined by

$$\omega_p^2 := 2edj_c/(\hbar\epsilon_0). \quad (9)$$

The second one is the so-called characteristic frequency defined by

$$\omega_c := (2eV_c/\hbar). \quad (10)$$

Here V_c is the voltage where the quasiparticle current density equals the value j_c . It is of the order of the superconducting energy gap and is a measure of the dissipative properties of the junction. In our simple model with a constant conductivity we have $\omega_c = 2edj_c/(\hbar\sigma)$. The ratio $\beta_c = \omega_c^2/\omega_p^2$ is the McCumber parameter. For the strongly anisotropic cuprate-superconductors $\beta_c \gg 1$ and we have phonons with $\omega_p < \omega_{\text{phon}} < \omega_c$.

Typically the time-dependence of the phase difference $\gamma(t)$ can be written in the so-called resistive state as

$$\gamma(t) = \theta + \omega t + \delta\gamma(t) \quad (11)$$

where $\omega = \langle \dot{\gamma} \rangle$ is the time-average of the phase velocity which is non-zero for a junction in the resistive state. It determines the dc-voltage $V = \langle E \rangle d = \hbar\langle \dot{\gamma} \rangle / (2e)$ across

the junction. In the steady state and for large values of the McCumber parameter β_c the oscillating part $\delta\gamma(t)$ is small and oscillates with the same frequency ω .

Now let us turn to the discussion of lattice vibrations. Note that the vibrating ions may be both in the barrier material and on the superconducting layers. The superconducting electrons are assumed to move together with the ions on the layers.

Quite generally the lattice displacement of an ion of type κ with mass M_κ , charge Z_κ in unit cell l is determined by the following equation of motion

$$M_\kappa \ddot{u}_\alpha(l_\kappa | t) + \sum_{l' \kappa'} \Phi_{\alpha\beta}(l_\kappa l' \kappa') u_\beta(l' \kappa' | t) = Z_\kappa E_\alpha^\rho(l_\kappa | t). \quad (12)$$

Here $E_\alpha^\rho(l_\kappa | t)$ is the local driving field at the equilibrium position $\vec{R}(l_\kappa) = \vec{R}(l) + \vec{R}(\kappa)$ of the ion generated by the charge fluctuations $\delta\rho_n(t)$ on the superconducting layers.

While the RSJ-equations for the phases are highly nonlinear, the relations between lattice displacements and electric fields are linear, consequently we may analyse the response for each frequency ω separately. With a harmonic ansatz of the form $u_z(l_\kappa | t) = u_z(l_\kappa) e^{-i\omega t}$ we obtain for the amplitude

$$u_z(l_\kappa) = \frac{1}{N} \sum_{\vec{q}\lambda} \sum_{l' \kappa'} \frac{e_z(\kappa | \vec{q}\lambda) e_z^*(\kappa' | \vec{q}\lambda)}{\omega^2(\vec{q}\lambda) - \omega^2} \times \frac{e^{i\vec{q}(\vec{R}(l_\kappa) - \vec{R}(l' \kappa'))}}{\sqrt{M_\kappa M_{\kappa'}}} Z_{\kappa'} E_z^\rho(l' \kappa'). \quad (13)$$

Here $\omega^2(\vec{q}\lambda)$ and $\vec{e}(\kappa | \vec{q}\lambda)$ are the eigenvalues and eigenvectors of the dynamical matrix

$$\sum_{\kappa' \beta} D_{\alpha\beta}(l_\kappa \vec{q}) e_\beta(\kappa' | \vec{q}\lambda) = \omega^2(\vec{q}\lambda) e_\alpha(\kappa | \vec{q}\lambda) \quad (14)$$

defined by

$$D_{\alpha\beta}(l_\kappa \vec{q}) = \sum_{l'} \frac{1}{\sqrt{M_\kappa M_{\kappa'}}} \Phi_{\alpha\beta}(l_\kappa l' \kappa') e^{i\vec{q}(\vec{R}(l' \kappa') - \vec{R}(l_\kappa))}. \quad (15)$$

The force-constant matrix contains the quantum-mechanical short-range interactions but also the short-range and long-range Coulomb interactions (the latter being of the form $q_\alpha q_\beta / q^2$) between the ions, but not the fields set-up by the conduction electrons on the layers. The eigenfrequencies $\omega(\vec{q}\lambda)$ are therefore by construction the *bare* phonon frequencies in the absence of the electronic charge fluctuations $\delta\rho_n(t)$.

For the further discussion it is convenient to label the lattice dynamical unit cells by $l = (l_x, l_y, l_z)$ with $l_z = n$ denoting the superconducting layer in which the lattice cell is contained (see Fig. 1). Then the z -component of the position vector $\vec{R}(l_\kappa)$ for $l = (l_x, l_y, n)$ does not depend on $l_\parallel = (l_x, l_y)$ and we may write

$R_z(l_\kappa) = R_z(n_\kappa) = R_z(n) + R_z(\kappa)$. Furthermore the origin of the unit-cell may be chosen on the superconducting layer, so that $R_z(n) = z_n$.

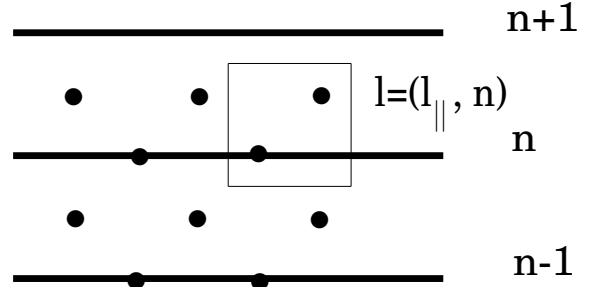


FIG. 1. Numbering of unit cells.

Note that the electric field $E_z^\rho(l_\kappa)$ and hence the ionic displacement in Eq. (13) do not depend on the position l_\parallel along the layer. Therefore in Eq. (13) only modes with $q_\parallel = 0$ appear, and we may write for the displacement amplitude of an ion of type κ in barrier n

$$u_z(n_\kappa) = \frac{1}{N_z} \sum_{q_z \lambda} \sum_{n' \kappa'} \frac{e_z(\kappa | q_z \lambda) e_z^*(\kappa' | q_z \lambda)}{\omega^2(q_z \lambda) - \omega^2} \times \frac{e^{i q_z (R_z(n_\kappa) - R_z(n_\kappa'))}}{\sqrt{M_\kappa M_{\kappa'}}} Z_{\kappa'} E_z^\rho(n_\kappa'). \quad (16)$$

Now let us specify the driving field $E_z^\rho(n_\kappa)$ for the ions in more detail: Summing up the electric fields created by the charge fluctuations on the different layers we find:

$$E_z^\rho(n_\kappa) = \begin{cases} \frac{1}{2\epsilon_0} \left(\sum_{n' \leq n} \delta\rho_{n'} - \sum_{n' > n} \delta\rho_{n'} \right) & \text{for } \kappa \in \text{barrier} \\ \frac{1}{2\epsilon_0} \left(\sum_{n' < n} \delta\rho_{n'} - \sum_{n' > n} \delta\rho_{n'} \right) & \text{for } \kappa \in \text{layer}. \end{cases} \quad (17)$$

Note that for ions *inside* the barrier the driving field does not depend on the position κ of the ion and is equal to the constant field E_n^ρ introduced in Eq. (4):

$$E_z^\rho(n_\kappa) = \begin{cases} E_n^\rho & \text{for } \kappa \in \text{barrier} \\ \frac{1}{2}(E_n^\rho + E_{n-1}^\rho) & \text{for } \kappa \in \text{layer}. \end{cases} \quad (18)$$

In order to find a relation between the lattice displacements and the driving field we introduce the Fourier transformation

$$E^\rho(q_z) = \sum_n E_z^\rho(n) e^{-i q_z z_n}. \quad (19)$$

Then

$$\sum_n Z_\kappa E_z^\rho(n_\kappa) e^{-i q_z R_z(n_\kappa)} =: \tilde{Z}_\kappa^* E^\rho(q_z) \quad (20)$$

where

$$\tilde{Z}_\kappa = \begin{cases} Z_\kappa e^{i q_z R_z(\kappa)} & \text{for } \kappa \in \text{barrier} \\ \frac{1}{2} Z_\kappa e^{i q_z R_z(\kappa)} (1 + e^{i q_z d}) & \text{for } \kappa \in \text{layer} \end{cases} \quad (21)$$

and consequently

$$u_z(\kappa) = \frac{1}{N_z} \sum_{q_z \lambda} \sum_{\kappa'} e^{iq_z R_z(\kappa)} \times \frac{1}{\sqrt{M_\kappa}} \frac{e_z(\kappa|q_z \lambda) e_z^*(\kappa'|q_z \lambda)}{\omega^2(q_z \lambda) - \omega^2} \frac{\tilde{Z}_{\kappa'}^*}{\sqrt{M_{\kappa'}}} E^\rho(q_z). \quad (22)$$

Thereby the vanishing of \tilde{Z}_κ for $q_z d = \pi$ and for ions on the layers reflects the fact that for alternating electric fields in the barriers no net force is acting on the superconducting layers.

Next we have to analyse the average total electric field E_n in the barrier. It is the field set-up by both the charge-fluctuations and the displaced ionic charges (we assume that in equilibrium the average electric field vanishes), $E_n = E_n^\rho + E_n^{\text{ion}}$. E_n^{ion} can be calculated (as shown in the Appendix) from the difference of the scalar potentials on layers n and $n+1$ produced by the ionic displacements as (v_c is the volume of one unit cell):

$$E_n^{\text{ion}} = -\frac{1}{\epsilon_0 v_c} \left(\sum_{\kappa \in \text{barrier}} Z_\kappa u_z(\kappa) + \frac{1}{2} \sum_{\kappa \in \text{layer}} Z_\kappa (u_z(\kappa) + u_z(\kappa+1)) \right). \quad (23)$$

Note that this field in the present case (for $q_{\parallel} = 0$) does not depend on the ionic displacements in other barriers and is closely related to the ionic polarisation. Therefore we define a generalised polarisation by

$$P_n := -\epsilon_0 E_n^{\text{ion}}, \quad (24)$$

and can write for the displacement in the barrier

$$D_n = \epsilon_0 E_n^\rho = \epsilon_0 E_n + P_n. \quad (25)$$

Going over to a Fourier transformation the relation

$$P(q_z) = \chi(q_z, \omega) \epsilon_0 E^\rho(q_z) \quad (26)$$

between the polarisation and the driving field is obtained with

$$\chi(q_z, \omega) = \sum_{\lambda} \frac{|\Omega(q_z \lambda)|^2}{\omega^2(q_z \lambda) - \omega^2} \quad (27)$$

and the oscillator strength

$$|\Omega(q_z \lambda)|^2 = \frac{1}{v_c \epsilon_0} \sum_{\kappa \kappa'} \tilde{Z}_\kappa \frac{e_z(\kappa|q_z \lambda) e_z^*(\kappa'|q_z \lambda)}{\sqrt{M_\kappa M_{\kappa'}}} \tilde{Z}_{\kappa'}^*. \quad (28)$$

The special combination of phase factors contained in \tilde{Z}_κ Eq. (21) are a consequence of the different contribution of ions on and between the superconducting layers to the electric field in the barrier.

Using $\epsilon_0 E^\rho(q_z) = \epsilon_0 E(q_z) + P(q_z)$ we can solve for $P(q_z)$:

$$P(q_z) = \frac{\chi(q_z, \omega)}{1 - \chi(q_z, \omega)} \epsilon_0 E(q_z). \quad (29)$$

The relation $D(q_z) = \epsilon_0 \epsilon_{\text{ph}}^L(q_z, \omega) E(q_z)$ defines an effective longitudinal dielectric function

$$\epsilon_{\text{ph}}^L(q_z, \omega) = \frac{1}{1 - \chi(q_z, \omega)} \quad (30)$$

This function has zeros at the eigenfrequencies $\omega(q_z \lambda)$ of the dynamical matrix. Due to the form of the oscillator strengths Eq. (28) only modes with polarization in c -direction contribute. As the electric field E_n is constant along the layers we have $\tilde{q}_{\parallel} = 0$ and only longitudinal modes in c -direction couple, therefore the zeros of $\epsilon_{\text{ph}}^L(q_z, \omega)$ are exactly at the longitudinal eigenfrequencies of the dynamical matrix.

In the case of a single dispersionless phonon-mode with frequency ω_L the function $\epsilon_{\text{ph}}^L(\omega)$ can be directly compared with the dielectric function used in Ref. 6. In fact, in this case $\epsilon_{\text{ph}}^L(\omega)$ can be written as

$$\epsilon_{\text{ph}}^L(\omega) = 1 + \frac{\Omega^2}{\omega_L^2 - \Omega^2 - \omega^2}. \quad (31)$$

In the general case the form of the longitudinal dielectric function Eq. (30) is different from the transverse dielectric function encountered usually in optical experiments, which is of the form $\epsilon_{\text{ph}}^T(\vec{q}, \omega) = 1 + \chi(\vec{q}, \omega)$. The latter is positive in the limit $\omega \rightarrow 0$, while $\epsilon_{\text{ph}}^L(\omega)$ can even become negative in the limit $\omega \rightarrow 0$, if the sum of oscillator strengths is sufficiently large.

Both functions can be combined to a general formula for the dielectric function (if we allow a lattice-polarisation in c -direction only):¹⁶

$$\epsilon_{\text{ph}}(\vec{q}, \omega) = 1 + \frac{\chi(\vec{q}, \omega)}{1 - f(\vec{q}) \chi(\vec{q}, \omega)}. \quad (32)$$

Here $\chi(\vec{q}, \omega)$ is a generalisation of the susceptibility Eq. (27) to arbitrary wave vectors $\vec{q} = (q_{\parallel}, q_z)$, and $f(\vec{q})$ is a function with the limits $f(q_{\parallel}, q_z) \rightarrow 1$ for $q_z \neq 0, q_{\parallel} \rightarrow 0$ and $f(q_{\parallel}, q_z) \rightarrow 0$ for $q_{\parallel} \neq 0, q_z \rightarrow 0$. In these limits the correct form of a longitudinal and transverse dielectric function is obtained.

The distinction between transverse and longitudinal dielectric functions is important for the interpretation of experimental results. The reflectivity edge for light polarised in c -direction is given by the frequency $\omega_{\text{cut-off}} = \omega_p / \sqrt{\epsilon_{\text{ph}}^T(0)}$ were ω_p is the bare Josephson plasma frequency. In the cuprate-superconductors values of $\epsilon_{\text{ph}}^T(0) = 12$ are estimated. This has to be considered if one wants to determine the bare plasma frequency ω_p from reflectivity experiments. On the other hand, longitudinal plasma oscillations are determined by the (different) frequency $\omega_p / \sqrt{|\epsilon_{\text{ph}}^L(0)|}$.

In addition let us briefly mention the influence of a background dielectric constant. There are two different effects to be considered:

1. We may want to treat the phonons with low frequency explicitly and describe the polarisation of high frequency phonons by a constant susceptibility χ_∞ . In that case we write

$$P_{\text{ph}} = \epsilon_0 \chi(\omega) E^\rho \quad (33)$$

and split the susceptibility

$$\chi(\omega) = \chi_{\text{low}}(\omega) + \chi_\infty \quad (34)$$

into a contribution from low frequency and high frequency phonons. Then defining $D = \epsilon_0 \epsilon_{\text{ph}}^L E$ we obtain

$$\epsilon_{\text{ph}}^L(\omega) = \frac{\epsilon_\infty}{1 - \chi_{\text{low}}(\omega) \epsilon_\infty} \quad (35)$$

with $\epsilon_\infty = 1/(1 - \chi_\infty)$.

2. We may want to include the effect of the polarisation due to other degrees of freedom, for instance an additional polarisation P_{el} due to bound electrons. With $D = \epsilon_0 E + P_{\text{ph}} + P_{\text{el}} = \epsilon_0 \epsilon^L E$ and an ansatz $P_{\text{el}} = \epsilon_0 \chi_{\text{el}} E$ we obtain

$$\epsilon^L(\omega) = \frac{\epsilon_\infty}{1 - \chi_{\text{ph}}(\omega)} \quad (36)$$

with $\epsilon_\infty = 1 + \chi_{\text{el}}$.

The two results are formally different. Note that in the first case the susceptibility χ_∞ relates the polarisation to the driving field E^ρ . In the second case χ_{el} relates the polarisation to the total field E . In the second case we have also to consider that the dynamical matrix for the phonon system is changed if we include an electronic polarisation.

Finally a comparison of our theory with theoretical investigations in Ref. 17 are in order. In principle there are two different electron-phonon coupling mechanisms, which may couple Josephson oscillations and phonons: 1. the electromagnetic interaction between the ionic charges and the charges of conduction electrons, 2. the dependence of the tunneling matrix element on lattice displacements. The first mechanism is considered in our work, the second in Ref. 17. Both mechanisms require a different theoretical treatment (on a diagrammatical basis the two mechanisms would correspond to different diagrams). It has been argued in Ref. 18 that in the layered cuprate superconductors the charges of the ions in the insulating barrier between superconducting layers are unscreened and therefore have a strong interaction with conduction electrons in the CuO₂-layers. We therefore considered this mechanism for our treatment of the coupling between Josephson oscillations and phonons. Though we did not write down a Hamiltonian for the interacting system our method nevertheless is a full microscopic theory which treats the electron-phonon interaction on a random-phase-type level by describing the interaction with help of internal fields. This approximation is sufficient as long as we do not want to consider the electron-phonon interaction inside the superconducting layers and treat exchange effects between different superconducting layers.

III. INFLUENCE OF PHONONS ON THE IV-CHARACTERISTIC

According to the RSJ-like model derived in Eq. (6) the current density in junction n is

$$j = j_c \sin \gamma_n(t) + \sigma E_n(t) + \dot{D}_n(t) \quad (37)$$

where $D_n(t) = \epsilon_0 E_n^\rho(t)$ is the electric field in junction n set-up by the charge fluctuations of conduction electrons. As pointed out in the previous section this field can be expressed by the average electric field in the barrier and the generalized polarisation Eq. (24) as $D_n(t) = \epsilon_0 E_n(t) + P_n(t)$. The polarisation has to be calculated self-consistently from the ionic displacements and depends linearly on the electric field.

Let us discuss first the case of one resistive junction at $n = 0$ in the middle of a large stack while all other junctions $n \neq 0$ are in the superconducting state. Then as mentioned previously all the oscillations are governed by one frequency ω , and we can write for the phase for $n = 0$:

$$\gamma_0(t) = \theta_0 + \omega t + \delta\gamma_0(t), \quad (38)$$

while for $n \neq 0$ we have

$$\gamma_n(t) = \theta_n + \delta\gamma_n(t). \quad (39)$$

In the stationary state $\delta\gamma_n(t)$ oscillates with the same frequency ω ,

$$\delta\gamma_n(t) = \delta\gamma_n e^{-i\omega t} + c.c. \quad (40)$$

Higher harmonics can be neglected for $\beta_c \gg 1$. In this limit the $\delta\gamma_n(t)$ are small and we may use the expansion

$$\sin \gamma_0(t) \simeq \sin(\theta_0 + \omega t) + \cos(\theta_0 + \omega t) \delta\gamma_0(t), \quad (41)$$

while for $n \neq 0$ we have

$$\sin \gamma_n(t) \simeq \sin \theta_n + \cos \theta_n \delta\gamma_n(t). \quad (42)$$

The bias current density j on the l.h.s. of the RSJ-equations Eq. (37) is time-independent and equal for all junctions, while the quantities on the r.h.s have both time-independent and oscillating components.

Let us discuss the equations for the non-resistive junctions ($n \neq 0$) first. Here the dc-component is:

$$j = j_c \sin \theta_n \quad (43)$$

This fixes the constant part of the phases in the non-resistive junctions and relates it to the bias current.

For the oscillating part of Eq. (37) one obtains:

$$0 = j_c \cos \theta_n \delta\gamma_n(t) + \sigma \frac{\hbar}{2ed} \delta\dot{\gamma}_n(t) + \dot{D}_n(t) \quad (44)$$

or

$$0 = \bar{\omega}_p^2 \delta\gamma_n(t) + \frac{\sigma}{\epsilon_0} \delta\dot{\gamma}_n(t) + \frac{2ed}{\hbar} \dot{D}_n(t) \quad (45)$$

with the reduced Josephson plasma frequency

$$\bar{\omega}_p^2 = \omega_p^2 \sqrt{1 - (j/j_c)^2}. \quad (46)$$

Now we discuss the resistive junction at $n = 0$. Keeping only the lowest harmonic we find

$$\sin \gamma_0(t) \simeq \sin(\theta_0 + \omega t) + \text{Real}(\delta\gamma_0 e^{i\theta_0}). \quad (47)$$

The dc-component of the RSJ-equation Eq. (37) is therefore given by

$$j(V) = j_{qp}(V) + j_c \text{Real}(\delta\gamma_0 e^{i\theta_0}), \quad (48)$$

where V is the dc-voltage of the resistive junction and $j_{qp}(V) = \sigma E_{dc}$ is the quasiparticle current density.

For the oscillating part one finds:

$$0 = j_c \sin(\theta_0 + \omega t) + \sigma \frac{\hbar}{2ed} \delta\dot{\gamma}_0(t) + \dot{D}_0(t). \quad (49)$$

The two equations (44, 49) can be combined to one inhomogeneous linear differential equation for all n

$$\bar{\omega}_p^2 \delta\gamma_n(t) + \frac{\sigma}{\epsilon_0} \delta\dot{\gamma}_n(t) + \frac{2ed}{\hbar} \dot{D}_n(t) = f_n(t) \quad (50)$$

with

$$f_n(t) = \begin{cases} \bar{\omega}_p^2 \delta\gamma_0(t) - \omega_p^2 \sin(\theta_0 + \omega t) & \text{for } n = 0 \\ 0 & \text{for } n \neq 0. \end{cases} \quad (51)$$

Assuming a time dependence of the form $e^{-i\omega t}$ for all oscillating functions we have

$$\bar{\omega}_p^2 \delta\gamma_n + \frac{-i\omega\sigma}{\epsilon_0} \delta\gamma_n + \frac{2ed}{\hbar} (-i\omega) D_n = f_n \quad (52)$$

with

$$f_n = \begin{cases} \bar{\omega}_p^2 \delta\gamma_0 - \frac{i\omega_p^2}{2} e^{-i\theta_0} & \text{for } n = 0 \\ 0 & \text{for } n \neq 0. \end{cases} \quad (53)$$

In order to incorporate the non-local dependence of the polarisation on the electric fields in different barriers a spatial Fourier representation of the form

$$\delta\gamma_n = \frac{1}{N_z} \sum_{q_z} \gamma(q_z) e^{iq_z z_n} \quad (54)$$

is introduced. Using the relation

$$D(q_z) = \epsilon_0 \epsilon_{\text{ph}}^L(q_z, \omega) E(q_z) = \frac{\epsilon_0 \hbar}{2ed} \epsilon_{\text{ph}}^L(q_z, \omega) (-i\omega) \gamma(q_z) \quad (55)$$

in Eq. (52) yields

$$G^{-1}(q_z, \omega) \gamma(q_z) = f_0 \quad (56)$$

with

$$G^{-1}(q_z, \omega) = \bar{\omega}_p^2 - i\omega \frac{\sigma}{\epsilon_0} - \omega^2 \epsilon_{\text{ph}}^L(q_z, \omega). \quad (57)$$

For the phase oscillation in the resistive junction follows

$$\delta\gamma_0 = \frac{1}{N_z} \sum_{q_z} \gamma(q_z) = g(\omega) f_0 \quad (58)$$

with

$$g(\omega) = \frac{1}{N_z} \sum_{q_z} G(q_z, \omega). \quad (59)$$

Solving for $\delta\gamma_0$

$$\delta\gamma_0 = \frac{1}{2} \frac{-i\omega_p^2}{g^{-1}(\omega) - \bar{\omega}_p^2} e^{-i\theta_0} \quad (60)$$

we obtain

$$\text{Real}(\delta\gamma_0 e^{i\theta_0}) = \frac{1}{2} \text{Im} \frac{\omega_p^2}{g^{-1}(\omega) - \bar{\omega}_p^2}. \quad (61)$$

From this finally the following expression for the dc-current density as function of the dc voltage is obtained:

$$\begin{aligned} j(V) &= j_{qp}(V) - \frac{j_c}{2} \frac{\omega_p^2}{\omega^2} \text{Im} \frac{1}{\tilde{\epsilon}(\omega)} \\ &= j_{qp}(V) + \frac{j_c}{2} \frac{\omega_p^2}{\omega^2} \frac{\tilde{\epsilon}_2(\omega)}{\tilde{\epsilon}_1^2(\omega) + \tilde{\epsilon}_2^2(\omega)}. \end{aligned} \quad (62)$$

Here $\tilde{\epsilon}(\omega)$ is a modified dielectric function

$$\tilde{\epsilon}(\omega) = \bar{\epsilon}_{\text{ph}}(\omega) + \frac{i\sigma}{\epsilon_0 \omega} \quad (63)$$

where

$$\bar{\epsilon}_{\text{ph}}(\omega) = J^{-1}(\omega) + \frac{\bar{\omega}_p^2}{\omega^2} - \frac{i\sigma}{\epsilon_0 \omega} \quad (64)$$

and

$$J(\omega) = \frac{1}{N_z} \sum_{q_z} \left[\epsilon_{\text{ph}}^L(q_z, \omega) - \frac{\bar{\omega}_p^2}{\omega^2} + \frac{i\sigma}{\epsilon_0 \omega} \right]^{-1}. \quad (65)$$

This expression describes the dc-current density as function of the dc-voltage $V = \hbar\omega/(2e)$. It has a maximum for frequencies ω where the real part $\tilde{\epsilon}(\omega)$ vanishes, i.e. for longitudinal phonon frequencies.

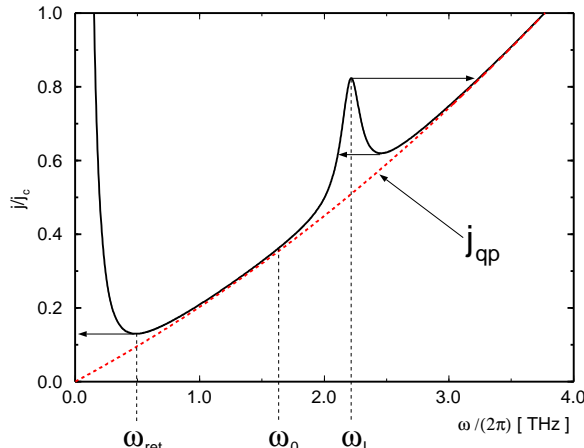


FIG. 2. Analytical I - V -curve for one resistive junction with one phonon resonance at $\omega = \omega_L$. The arrows mark the hysteretic jumps found in current-biased experiments and numerical simulations.

This can easily be seen if we consider the special case of one phonon mode without dispersion. Then $\bar{\epsilon}_{\text{ph}}(\omega) = \epsilon_{\text{ph}}^L(\omega)$, which is of the form Eq. (31). The corresponding I - V -curve is shown in Fig. 2, which is calculated with the dielectric function

$$\epsilon_{\text{ph}}^L(\omega) = 1 + \frac{\Omega^2}{\omega_L^2 - \Omega^2 - \omega^2 - i\omega\rho}. \quad (66)$$

Here an additional damping ρ of the phonon has been introduced in Eq. (31) in order to simulate the energy transfer into other junctions. A peak in the I - V -curve appears at $\omega = \omega_L$. The width of the peak is determined by this damping together with the quasiparticle conductivity. The deviation from the quasiparticle current density vanishes at the pole of $\epsilon_{\text{ph}}^L(\omega)$ at $\omega_0 = \sqrt{\omega_L^2 - \Omega^2}$. The rise at low voltages is due to the plasma resonance. For $\beta_c \gg 1$ the minimum of the I - V -curve is at $\omega_{\text{ret}} = (3/2)^{1/4}\omega_p/\sqrt{\epsilon_{\text{ph}}^L(0)}$. In current-biased experiments and in numerical simulations the parts with negative differential conductivity are skipped hysteretically as indicated in the figure.

Note that the denominator in the function $J(\omega)$ Eq. (65) is the total q_z - and ω -dependent longitudinal dielectric function of the coupled system of phonons and conduction electrons,

$$\epsilon_{\text{tot}}^L(q_z, \omega) = \epsilon_{\text{ph}}^L(q_z, \omega) - \frac{\bar{\omega}_p^2}{\omega^2} + \frac{i\sigma}{\epsilon_0\omega}. \quad (67)$$

Zeros of the real part of this function describe longitudinal collective modes in the system. On the other hand the resonances in the I - V curve appear at the *bare* longitudinal phonon frequency. The summation over q_z in Eq. (65) leads to an effective damping of the resonances which is proportional to the phonon dispersion. The physical origin is the transfer of energy by phonons from the resistive junction to the neighboring junctions.

The result for the current-voltage characteristic can be generalised to the case of several junctions being in the resistive state, if we assume that all junctions oscillate with the same frequency ω . Denoting the subset of indices for the resistive junctions by I then for $i \in I$ we obtain (for a derivation see the appendix):

$$j(V) = j_{qp}\left(\frac{\hbar\omega}{2e}\right) - \frac{j_c}{2} \frac{\omega_p^2}{\omega^2} \text{Im} \sum_{k \in I} e^{i\theta_i} \left[\bar{\epsilon}(i, k, \omega) + \frac{i\sigma}{\epsilon_0\omega} \delta_{i,k} \right]^{-1} e^{-i\theta_k} \quad (68)$$

The dielectric function $\bar{\epsilon}(i, k, \omega)$ is defined by

$$\bar{\epsilon}(i, k, \omega) := \left[\frac{1}{N_z} \sum_{q_z} \frac{e^{iq_z(z_i - z_k)}}{\epsilon_{\text{ph}}^L(q_z, \omega) - \frac{\bar{\omega}_p^2}{\omega^2} + \frac{i\sigma}{\epsilon_0\omega}} \right]^{-1} + \left(\frac{\bar{\omega}_p^2}{\omega^2} - \frac{i\sigma}{\epsilon_0\omega} \right) \delta_{i,k} \quad (69)$$

The brackets in Eqs. (68, 69) are understood as matrix inversions. The dc-voltage V is obtained, if one multiplies $\hbar\omega/(2e)$ by the number of resistive junctions. Note that the r.h.s. of Eq. (68) depends on the layer index i , while the l.h.s. is equal for each junction. From this equality the (relative) phases in the different junctions can be determined.

In the case of two resistive junctions exactly two solutions exist with $\theta_i = \theta_j$ and $\theta_i = \theta_j + \pi$, respectively. In the general case several different solutions are found. The stability of these solutions will be checked by a comparison with a direct numerical integration of the coupled equations of motions in the following section. It turns out, that those analytical solutions are most stable where the phases θ_i of the oscillating Josephson junctions fit best to the pattern of lattice vibrations.

IV. A SIMPLE EXAMPLE

In this section we want to illustrate the results of our theory for the most simple lattice dynamical model describing longitudinal modes in c -direction with one acoustical and one optical band: a lattice of two kinds of ions with ionic charges Z_l , $Z_b = -Z_l$ and masses M_l , M_b . The first kind ($\kappa = l$) is placed on the superconducting layers, the second kind ($\kappa = b$) in the middle of the barrier. The motion of ions in c -direction which is assumed to be uniform along the layers is approximated by a two-atomic chain-model with next-neighbor interactions in c -direction:

$$M_l \ddot{u}_l^{(n)} - f(u_b^{(n)}) + u_b^{(n-1)} - 2u_l^{(n)}) = Z_l E^{\rho}(l) \\ M_b \ddot{u}_b^{(n)} - f(u_l^{(n+1)}) + u_l^{(n)} - 2u_b^{(n)}) = Z_b E^{\rho}(b) \quad (70)$$

By choosing the masses very different a narrow optical band can be simulated which is found in cuprate superconductors. From a diagonalisation of the dynamical matrix given by Eq. (70) the well-known eigenfrequencies

$\omega(q_z\lambda)$ of the two-atomic chain are obtained. With help of the eigenvectors the oscillator strengths defined in Eq. (28) are calculated, which are needed for the longitudinal dielectric function Eq. (30).

The driving field on the r.h.s. of Eq. (70) is the field set-up by the conduction electron charges on the superconducting layers, which can be expressed by the (constant) field E_n^ρ in the barrier between layers n and $n+1$ with the help of Eq. (18). The latter can be expressed by the average total electric field E_n in the barrier:

$$E_n^\rho = E_n + \frac{1}{\epsilon_0} P_n \quad (71)$$

where the polarisation Eq. (24) is given by:

$$P_n = \frac{1}{v_c} \left(Z_b u_{,b}^{(n)} + \frac{1}{2} Z_l (u_{,l}^{(n)} + u_{,l}^{(n+1)}) \right) \quad (72)$$

These equations for the motion of lattice displacements have to be supplemented by the extended RSJ-equations Eq. (37):

$$j = j_c \sin \gamma_n(t) + \sigma \frac{\hbar}{2ed} \dot{\gamma}_n(t) + \epsilon_0 \frac{\hbar}{2ed} \ddot{\gamma}_n(t) + \dot{P}_n(t) \quad (73)$$

This model is used to calculate the I - V -characteristics in two ways: 1. The I - V -curves are calculated analytically using the results Eq. (68) obtained by the Green's function method. Thus the peaks due to the phonon resonances are obtained. 2. The coupled set of RSJ equations Eq. (73) and phonon equations Eqs. (70, 72) are integrated numerically by a Runge-Kutta method for a finite stack of Josephson junctions. Changing the bias-current gradually allows to follow the I - V -curves as in the current-biased experimental situation and to reproduce the hysteretic behaviour particularly.

We start with the discussion of the first branch of the I - V -curve, where one junction is in the resistive state.

A. One resistive junction

Quite generally the I - V -curve is expected to have peaks at the van Hove singularities of the phonon dispersion. Details, however, depend on the oscillator strength defined by Eq. (28) which enters the longitudinal dielectric function Eq. (30). In particular at the edge of the Brillouin zone for $q_z = \pi/d$ only the motion of ions within the barrier contribute to the oscillator strength, the ions on the superconducting layers are inactive due to the factor $1 + \exp(iq_z d)$ in Eq. (21).

These general principles are now applied to the lattice dynamical model introduced above. Here at $q_z = \pi/d$ only one type of particles is moving due to symmetry: In the acoustical branch the heavier ion, in the optical branch the lighter ion is moving. If the heavier ion is on the superconducting layers ($M_l > M_b$) the oscillator strength vanishes at the end of the acoustic branch

(see Fig. 3), and peaks are expected to appear in the I - V curve at the two van-Hove singularities of the optical branch. On the other hand, if the lighter ion is on the superconducting layers ($M_l < M_b$) then the oscillator strength vanishes at the end of the optical branch, and peaks are expected at $q_z = \pi/d$ from the acoustical branch and at $q_z = 0$ from the optical branch.

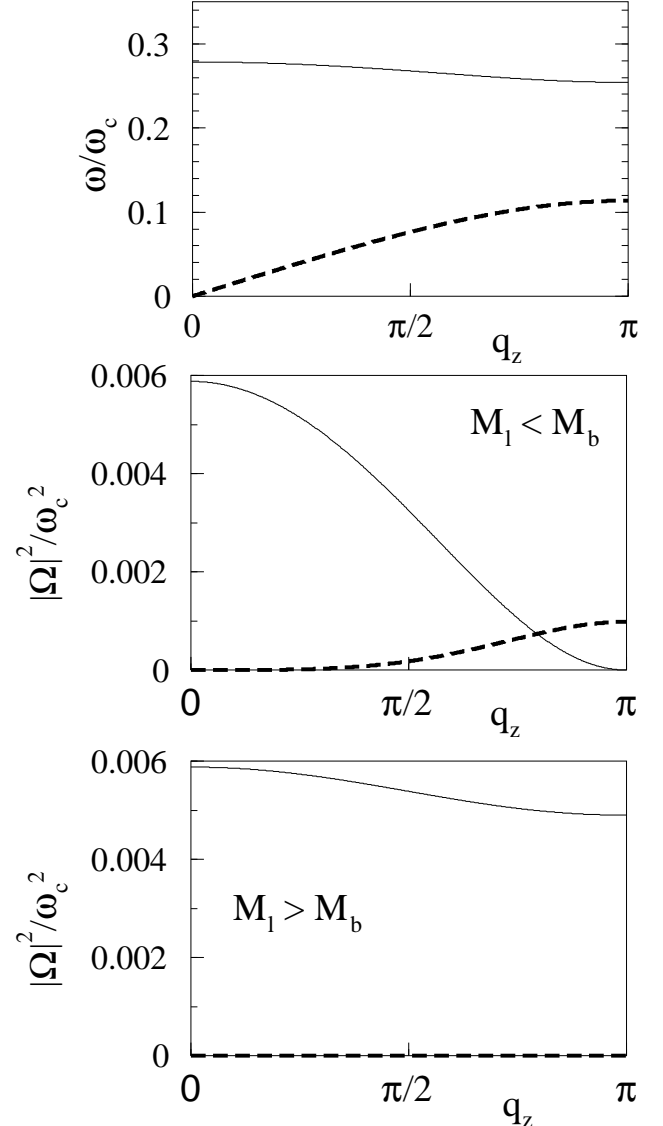


FIG. 3. Dispersion and oscillator strengths for the two-atomic chain model. Shown are the oscillator strengths $|\Omega(q_z\lambda)|^2$ for the acoustical branch (dashed curve) and the optical branch (solid curve) and for the two cases of the heavy ions on the superconducting layer ($M_l > M_b$) and in the barrier ($M_l < M_b$).

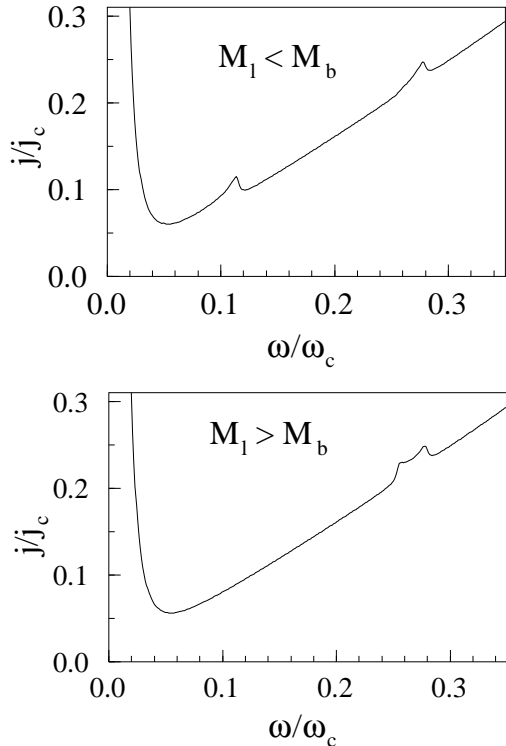


FIG. 4. *I-V*-curves for one resistive junction with supgap-structures due to acoustical and optical phonons.

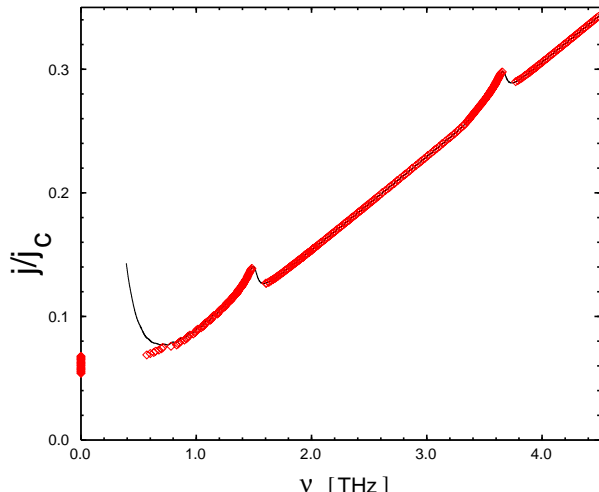


FIG. 5. Comparison between analytical (solid line) and numerical results (rhombi) for the *I-V*-curve of one resistive junction with supgap-structures due to acoustical and optical phonons for $M_l < M_b$.

This is illustrated in Fig. 4 where we have plotted results for the *I-V*-curve of the first branch in the two cases $M_l < M_b$ and $M_l > M_b$. In our model the phonon dispersion is fixed by the values of $\omega_{\text{LO}}^2(q_z = 0) = 2f(1/M_l + 1/M_b)$ and the mass ratio M_l/M_b . A measure for the oscillator strength is the quantity $\Omega_{l,b}^2 := Z^2/(M_{l,b}\epsilon_0 v_c)$. In Fig. 4 we have used the following parameters: $\beta_c = \omega_c^2/\omega_J^2 = 375$, $M_l/M_b = 0.2$ and

$M_b/M_l = 0.2$. The phonon frequencies are normalised to ω_c and are given by $\omega_{\text{LO}}(q_z = 0) = 0.28\omega_c$. The oscillator strength is given by $\omega_c^2/\Omega_l^2 = 200$ for $M_l < M_b$ and $\omega_c^2/\Omega_b^2 = 200$ for $M_l > M_b$. The corresponding phonon dispersion and the oscillator strengths are shown in Fig. 3.

For $M_l < M_b$ the analytical results for the *I-V*-curve in Fig. 4 show phonon peaks at the end of the acoustic branch at $q_z = \pi/d$ and at the van Hove singularity at $q_z = 0$ of the optical branch, while for $M_l > M_b$ only structures due to the two van Hove singularities of the optical branch appear. In both cases the increase at low frequencies indicates the Josephson plasma frequency. The numerical results shown in Fig. 5 for $M_l < M_b$ (here $\omega_c = 13.1\text{THz}$) follow the analytical results in the regions of positive differential resistance, and otherwise show the hysteretic behaviour as seen in experiments. At low values of j/j_c the *I-V*-curve switches back to the superconducting state of the junction.

B. Two resistive junctions

The second branch of the *I-V*-curve has a more complex structure already for one phonon band. This is shown schematically in Fig. 6. If we denote the two dynamical states of the first branch by *a* and *b*, then on the second branch with two resistive junctions either both junctions are in state *a* (label *aa*), both junctions are in state *b* (label *bb*) or one junction is in state *a* while the other junction is in state *b* (label *ab*). Note that in the latter case the oscillation frequencies of the two junctions are different. In the case of well separated resistive junctions the voltages of a structure for a given bias current are determined by $\omega_{aa} = 2\omega_a$, $\omega_{bb} = 2\omega_b$, $\omega_{ab} = \omega_a + \omega_b$. This is no longer true, if the resistive junctions are close to each other and interact via phonons. Then the voltages in the second branch are slightly lower.

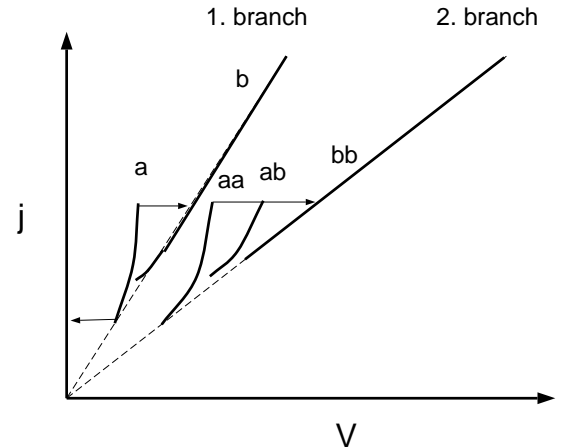


FIG. 6. Schematic plot of the first and second branch of the *I-V*-curve with subgap structures due to one phonon.

In the case of two resistive junctions i and j two solutions of Eq. (68) exist with phase differences $\theta_i = \theta_j$ and $\theta_i = \theta_j + \pi$, corresponding to in-phase and out-of-phase Josephson oscillations, respectively. Inserting these results in Eq. (68) two different I - V -curves can be calculated. Note that this formula applies only for the states aa and bb , because in the derivation we have assumed that the two junctions oscillate with the same frequency. A similar formula can also be derived for the state ab . In that case the solution does not depend on the phases.

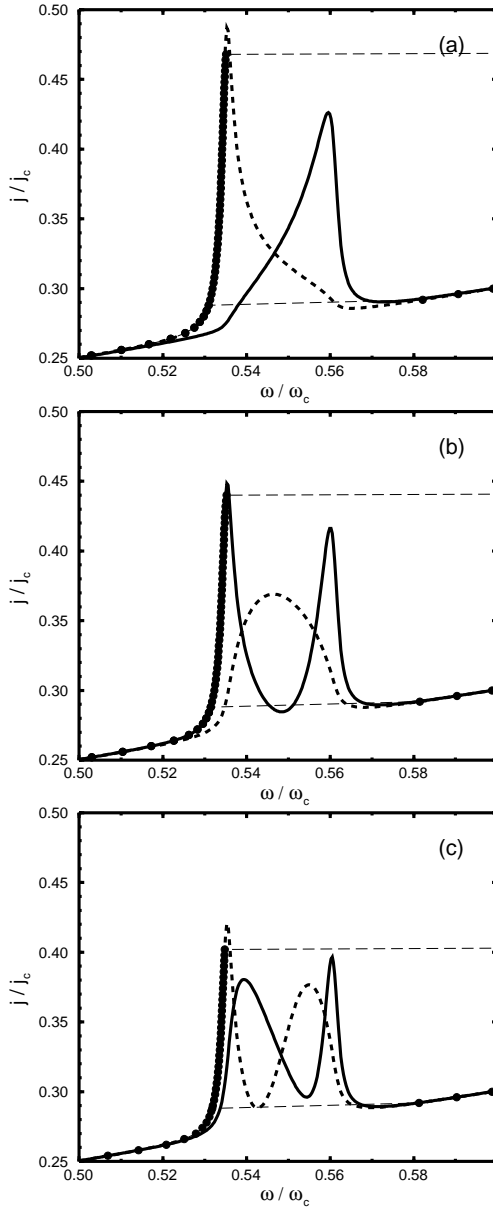


FIG. 7. I - V -curve for two resistive junctions separated by 0 (a), 1 (b), 2 (c) superconducting junctions. Shown are analytical I - V -curves calculated for a narrow optical band for the in-phase, $\theta_j - \theta_i = 0$ (solid line) and the out-of-phase, $\theta_j - \theta_i = \pi$ (dashed line) solution together with numerical results.

In Fig. 7 we show examples calculated for a narrow optical band with $M_l/M_b = 10$ and the light ion oscillating in the barrier. Here the different analytical solutions are shown together with numerical results for neighboring resistive junctions, $j = i + 1$ (a), and two resistive junctions separated by 1 or 2 superconducting junctions, $j = i + 2$ (b), $j = i + 3$ (c).

It is plausible that in the case of neighboring resistive junctions out-of-phase Josephson oscillations favor a coupling to phonons at the edge of the Brillouin zone, while the coupling of in-phase oscillations is strongest for zone-center phonons. This is shown in Fig. 7a, where the I - V -curve for the in-phase solution shows a peak at $\omega(q_z = 0)$, while for the out-of-phase solution the current-maximum is at $\omega(q_z = \pi/d)$.

It can be seen that the numerical results in the dynamical state aa follow one of the analytical solutions before a hysteretic switch into state bb occurs (outside the figure). This is verified in Fig. 7a where the numerical I - V -curve follows the analytical curve for $\theta_i = \theta_{i+1} + \pi$. In Fig. 7b the in-phase solution with $\theta_i = \theta_{i+2}$ has maxima for voltages corresponding to frequencies of optical phonons at both $q_z = \pi/d$ and $q_z = 0$, while the out-of-phase solution has a broad maximum in the middle of the Brillouin zone. The numerical results follow the in-phase solution. Fig. 7c shows results for $j = i + 3$.

The results obtained for two resistive junctions show that the peak position in the I - V -curve depends only slightly on the distance between the resistive junctions. More important is the fact that phonons are able to synchronise the phases of Josephson oscillations in different resistive junctions. This is important for the use of such systems in high-frequency applications. In the case of many resistive junctions an optimal synchronisation is expected for the coupling with optical phonons at $q_z = 0$.

V. COMPARISON WITH EXPERIMENTAL RESULTS

Recently the explanation of the subgap resonances in Refs. 3–5,8 with the phonon coupling mechanism presented here could be well confirmed by Raman measurements on the same samples^{4,19} and infrared reflectivity experiments with grazing incidence,^{11,20} where the latter allows to determine both longitudinal and transverse modes (see Table I). Small deviations of the order of ~ 5 – 10% can be attributed to the fact that in optical experiments and in the intrinsic Josephson effect different averages over \vec{q} of the dielectric functions are relevant. Note that in our theory also modes which are Raman active at $q_z = 0$ may couple to intrinsic Josephson oscillations for $q_z \neq 0$. Earlier experimental data,^{9,10} which are obtained from polycrystalline samples, show the same qualitative behaviour, but differ in detail.

With the help of rigid-ion²¹ and shell-model calculations^{22–24} some of the more pronounced structures

can be connected with certain elongation patterns of the ions in the unit cell. For example, the peak in the I - V -curve at 4.64 THz in $\text{Tl}_2\text{Ba}_2\text{Ca}_2\text{Cu}_3\text{O}_{10}$ seems to be due to a (Cu,Ba)-mode.

The qualitative features of the subgap resonances have already been explained with the help of the phonon interpretation in Ref. 8: The position of the resonance is completely independent on temperature, magnetic field and the geometry of the probe, while the intensity of the structure varies $\sim j_c^2$ with the critical current density $j_c(T, B)$. Also the behaviour of the position and intensity of the structures in external pressure are in agreement with the phonon explanation and formula (1).

One of the main qualitative features of the general theory with dispersive phonon bands, which goes beyond the local oscillator model used in Refs. 6,8, is the possibility to describe resonances at van-Hove singularities, which appear e.g. at the upper band edge of the acoustical phonon band. This might be an explanation for a resonance seen in Ref. 5 at 3.2 mV (≈ 1.54 THz) in the I - V -characteristic of $\text{Tl}_2\text{Ba}_2\text{Ca}_2\text{Cu}_3\text{O}_{10}$, because the same frequency is expected by lattice dynamical calculations²³ for the upper edge of the acoustical band, and there are no optical phonon bands in this low frequency range. Fig. 8 shows a fit of a I - V -curve calculated with the two-atomic chain model (and some additional damping) to the experimental results from Ref. 5.

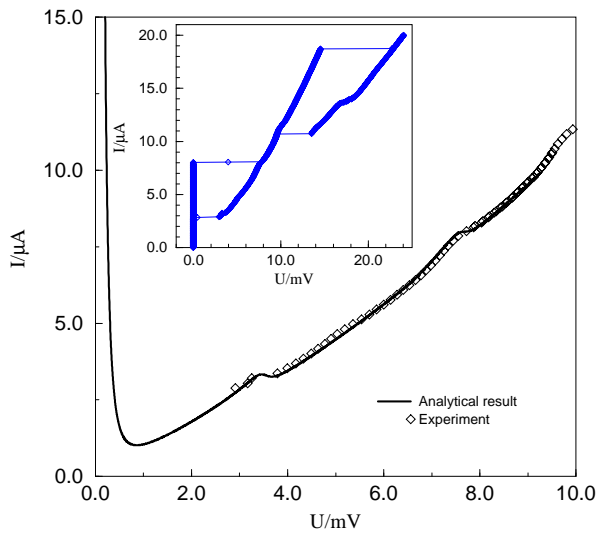


FIG. 8. Fit of the experimental I - V -curve in $\text{Tl}_2\text{Ba}_2\text{Ca}_2\text{Cu}_3\text{O}_{10}$ from Ref. 5 near the subgap resonances at the band edge of the acoustical branch (at 1.5 THz) and an optical branch with the help of the a two-atomic chain model. The inset shows experimental results over a wider frequency range.

Also the effect of the two van-Hove singularities at the optical band edges on the I - V -curve as discussed above might have been seen in the satellite structures at 5.17

THz (10.7 mV) and 5.6 (11.6 mV) in the I - V -curve of BSCCO⁷. This interpretation is further supported by the theoretical prediction of the bandwidth ~ 0.3 THz and the fact that the assignment of no other phonon mode is plausible.

TABLE I. Comparison of the frequencies $f_{\text{sg}} = \frac{\hbar}{2e}V_{\text{dc}}$ (in THz) of the most pronounced subgap resonances in Ref. 8 and of infrared- and Raman active modes in $\text{Bi}_2\text{Sr}_2\text{CaCu}_2\text{O}_8$ and $\text{Tl}_2\text{Ba}_2\text{Ca}_2\text{Cu}_n\text{O}_{2n+4}$.

Subgap Resonances and Phonons in $\text{Bi}_2\text{Sr}_2\text{CaCu}_2\text{O}_8$					
f_{sg}	2.97	3.89	5.17	5.60	Ref. 8
f_{LO}	2.85		5.07		Ref. 11
f_{LO}	2.86		5.16		Ref. 20
f_{TO}		3.80			Refs. 4,19
Subgap Resonances and Phonons in $\text{Tl}_2\text{Ba}_2\text{Ca}_2\text{Cu}_n\text{O}_{2n+4}$					
f_{sg}	3.63	4.64			Ref. 8
f_{LO}		4.50			Ref. 11
					Josephsoneffect ^a
					IR-reflecticity ^b

^a $\text{Tl}_2\text{Ba}_2\text{Ca}_2\text{Cu}_3\text{O}_{10}$

^b $\text{Tl}_2\text{Ba}_2\text{Ca}_2\text{O}_8$

VI. SUMMARY

In this paper we have developed a microscopic theory for the coupling between Josephson oscillations and phonons in intrinsic Josephson systems like the highly anisotropic cuprate superconductors. We determined the precise form of the longitudinal dielectric function Eq. (30) describing this coupling and obtained analytical results Eqs. (62,68) for the I - V -curve for one and several resistive junctions.

We have shown that not only optical phonons but also acoustical phonons at the edge of the Brillouin zone couple to Josephson oscillations. This may explain the structure observed in Ref. 5 in the I - V -curve occurring at an unusual low voltage (frequency), which is not found in reflectivity experiments, testing transverse optical phonons at $\vec{q} = 0$, and in lattice-dynamical calculations for infrared active phonons at $\vec{q} = 0$.

The analytical results are compared with results from a numerical integration of the coupled equations of motion for the Josephson oscillations and phonons. For this purpose a simplified lattice dynamical model has been used with one acoustical and one optical branch. It is found that in the limit of large values of the McCumber parameter the numerical results follow closely the analytical solutions with the following exceptions: 1. Using a gradual change of the bias-current, regions of the I - V -curve with negative differential conductivity are skipped as is observed in current-biased experiments. 2. In the case of several resistive junctions, where several analytical solutions are obtained, the numerical result follows one of the analytical solutions. The stability of the different analytical solutions is currently investigated. It seems to be that the solution which gives a minimum for the interaction energy between polarisation and the electric field generated by the Josephson oscillations at a given frequency is most stable. The phonons thus serve to synchronise the Josephson oscillations in different resistive layers, which is important for the application of such systems as high-frequency devices.

In this paper we have considered only the case of a current distribution in c-direction which is homogeneous along the layers. We neglected all magnetic field effects assuming that all quantities are uniform along the layers. For real systems this is an artificial approximation, because the current induced magnetic field cannot be avoided. Nevertheless, we argue that this is a valid approximation for the intrinsic Josephson systems forming a mesa structure of about hundred layers with a width of several μ and a thickness which is much smaller. Such a junction is still short with respect to the Josephson penetration depth $\lambda_J = c/\omega_p$ describing the possible variation of the phase-difference along the layers. Therefore the treatment of the superconducting layers as metal sheets with a uniform charge distribution, the creation of uniform polarisation fields and the neglect of q_{\parallel} in the calculation of the longitudinal dielectric function is fully justified.

This will be different in the case of longer junctions and strong external magnetic field. Then we have to consider also the penetration and flow of vortices and their interaction with phonons.

ACKNOWLEDGEMENT

The authors would like to thank A. Yurgens and A. Tsvetkov for discussions on their experimental results and for providing unpublished data, A. Mayer and D. Strauch for fruitful discussions on lattice dynamical aspects, and P. Müller and R. Kleiner for the permanent support of our work on intrinsic Josephson systems. Financial support by the Deutsche Forschungsgemeinschaft, the Bayerische Forschungsstiftung within the research project FORSUPRA and the Studienstiftung des Deutschen Volkes is gratefully acknowledged.

APPENDIX A: FIELD PRODUCED BY IONIC DISPLACEMENTS

In this Appendix we want to calculate the electric scalar potential on the superconducting layers and the electric field E^{ion} , which is produced by the displacement $\vec{u}(\vec{r})$ of the ions.

Quite generally this potential is given by

$$\Phi^{\text{ion}}(\vec{r}) = \frac{1}{4\pi\epsilon_0} \sum_{l' \kappa'} \frac{q_{\kappa}}{|\vec{R}(\vec{r}') + \vec{u}(\vec{r}') - \vec{r}|}. \quad (\text{A1})$$

Here \vec{r} is a coordinate vector on the superconducting layer. In principle we have to consider that also the superconducting layer is not only displaced but also possibly warped. However, in our theoretical description of the Josephson effect it is not possible to distinguish between different electronic sites on the layer within one unit cell. Therefore we are interested only in the electronic potential averaged over one unit cell in ab-direction:

$$\bar{\Phi}^{\text{ion}}(l_{\parallel}, n) = \frac{1}{F_c} \int_{F_c} d^2r \Phi^{\text{ion}}(\vec{r}). \quad (\text{A2})$$

Hence we write

$$\vec{r} = \vec{R}(l_{\parallel}, n) + \vec{u}(l_{\parallel}, n) + \vec{x} \quad (\text{A3})$$

where $\vec{R}(l_{\parallel}, n)$ and $\vec{u}(l_{\parallel}, n)$ are the equilibrium position and the average displacement of layer n in unit cell $l = (l_x, l_y, n) = (l_{\parallel}, n)$. The latter is given by

$$\vec{u}(l_{\parallel}, n) = \frac{1}{N_0} \sum_{\kappa \in \text{layer}} \vec{u}(\vec{r}_{\kappa}^{l_{\parallel}, n}). \quad (\text{A4})$$

Here the sum is over the N_0 ions on the superconducting layer within one unit cell. The vector \vec{x} denotes the

position on the layer in the unit cell and is now in the (x, y) -plane.

In the following we assume that the crystal is uncharged $\sum_{\kappa} Z_{\kappa} = 0$ and there is no polarisation in the equilibrium $\sum_{\kappa} Z_{\kappa} \vec{R}(\kappa) = 0$.

Expanding Eq. (A1) with respect to small lattice displacements we obtain for the potential change $\delta\bar{\Phi}^{\text{ion}}(l_{\parallel}, n) = \bar{\Phi}^{\text{ion}}(l_{\parallel}, n) - \Phi(n)$

$$\delta\bar{\Phi}^{\text{ion}}(l_{\parallel}, n) = \frac{1}{4\pi\epsilon_0} \frac{1}{F_c} \sum_{l' \kappa'} \int_{F_c} d^2x Z_{\kappa'} \times \frac{(\vec{u}(\kappa') - \vec{u}(l_{\parallel}, n))(\vec{R}(l_{\parallel}, n) - \vec{R}(\kappa') + \vec{x})}{|\vec{R}(l_{\parallel}, n) - \vec{R}(\kappa') + \vec{x}|^3} \quad (\text{A5})$$

where the integration is over the surface F_c of one unit cell in ab-direction. For phonons with $q_{\parallel} = 0$ the potential does not depend on l_{\parallel} and the integration over x may be extended over the whole surface F of one layer. Extending the surface boundaries to infinity the integral can easily be performed

$$\int d^2x \frac{(\vec{R}(l_{\parallel}, n) - \vec{R}(\kappa') + \vec{x})}{|\vec{R}(l_{\parallel}, n) - \vec{R}(\kappa') + \vec{x}|^3} = -2\pi\hat{z}\text{sgn}(R_z(\kappa') - R_z(l_{\parallel}, n)) \quad (\text{A6})$$

with

$$\text{sgn}(R_z(\kappa') - R_z(l_{\parallel}, n)) = \begin{cases} +1 & \text{for } R_z(\kappa') - R_z(l_{\parallel}, n) > 0 \\ 0 & \text{for } R_z(\kappa') - R_z(l_{\parallel}, n) = 0 \\ -1 & \text{for } R_z(\kappa') - R_z(l_{\parallel}, n) < 0. \end{cases} \quad (\text{A7})$$

Then we obtain for the potential on layer n

$$\delta\bar{\Phi}^{\text{ion}}(n) = -\frac{1}{2\epsilon_0} \frac{1}{F} \sum_{l' \kappa'} Z_{\kappa'} (u_z(\kappa') - u_z(n)) \times \text{sgn}(R_z(\kappa') - R_z(n)). \quad (\text{A8})$$

For a neutral unit cell and in the absence of a static polarisation the contribution from $u_z(n)$ vanishes. Using furthermore that for $q_{\parallel} = 0$ the displacement $\vec{u}(\kappa')$ does not depend on l'_{\parallel} we obtain the simpler expression

$$\delta\bar{\Phi}^{\text{ion}}(n) = -\frac{1}{2\epsilon_0 v_c} \sum_{n' \kappa'} Z_{\kappa'} u_z(\kappa') \text{sgn}(R_z(\kappa') - R_z(n)), \quad (\text{A9})$$

where v_c is the volume of the unit cell.

The averaged electric field across one barrier between layers n and $n+1$ is given by the potential difference

$$E_n^{\text{ion}} = \frac{1}{d} \int_{z_n}^{z_{n+1}} E^{\text{ion}}(z) dz = \frac{1}{d} (\delta\bar{\Phi}^{\text{ion}}(n) - \delta\bar{\Phi}^{\text{ion}}(n+1)). \quad (\text{A10})$$

In this difference the contributions from lattice displacements of ions outside the barrier cancel, and we obtain for the field produced by the ionic displacements

$$E_z^{\text{ion}}(n) = -\frac{1}{\epsilon_0 v_c} \left(\sum_{\kappa \in \text{barrier}} Z_{\kappa} u_z(\kappa) + \frac{1}{2} \sum_{\kappa \in \text{layer}} Z_{\kappa} (u_z(\kappa) + u_z(\kappa+1)) \right). \quad (\text{A11})$$

The factor 1/2 in Eq. (A11) results from the fact that ionic displacements on the superconducting layers do not contribute to the potential on that layer. The electric field set-up by the ionic displacements contains contributions from displacements of ions in the barrier and from ions on the superconducting layers, which correspond to the macroscopic polarisation of the barrier. This will be different in the case $q_{\parallel} \neq 0$ where also lattice displacements in neighboring barriers contribute to the field in barrier n .

APPENDIX B: SEVERAL RESISTIVE JUNCTIONS

Quite generally the RSJ-equation for the n -th junction can be written as

$$j = j_c \sin \gamma_n(t) + \sigma \frac{\hbar}{2ed} \dot{\gamma}_n(t) + \frac{\epsilon_0 \hbar}{2ed} \sum_{n'} \int_{-\infty}^{\infty} \epsilon_{\text{ph}}^L(n, n', t - t') \ddot{\gamma}_{n'}(t') dt'. \quad (\text{B1})$$

where $\epsilon_{\text{ph}}^L(n, n', t)$ is the dielectric function Eq. (30) in real space and time domain.

Let us denote the index of a general junction by $n \in 1..N$ and the subset of indices of resistive junctions by I . In the following we assume that oscillations in all junctions are governed by one frequency ω and the phases can be written as

$$\gamma_n(t) = \begin{cases} \theta_j + \omega t + \delta\gamma_j(t) & n = j \in I \\ \theta_n + \delta\gamma_n(t) & \text{else} \end{cases} \quad (\text{B2})$$

with

$$\delta\gamma_n(t) = \delta\gamma_n e^{-i\omega t} + \text{c.c.} \quad (\text{B3})$$

From an expansion with respect to $\delta\gamma$ and keeping only the lowest harmonic one finds

$$\sin \gamma_n(t) \simeq \begin{cases} \sin(\theta_j + \omega t) + \text{Real}(\delta\gamma_j) e^{i\theta_j} & n = j \in I \\ \sin \theta_n + \cos \theta_n \delta\gamma_n(t) & \text{else.} \end{cases} \quad (\text{B4})$$

Splitting the RSJ-equation (B1) into a dc-part and an oscillating part one obtains for the dc-part:

$$j = \begin{cases} \sigma E_{dc} + j_c \text{Real}(\delta\gamma_j e^{i\theta_j}) & \text{for } n = j \in I \\ j_c \sin \theta_n & \text{else,} \end{cases} \quad (\text{B5})$$

while the oscillating part can be written as ($\bar{\omega}_p^2 = \omega_p^2 \sqrt{1 - (j/j_c)^2}$)

$$\begin{aligned} \bar{\omega}_p^2 \delta \gamma_n(t) + \frac{\sigma}{\epsilon_0} \delta \dot{\gamma}_n(t) \\ + \sum_{n'} \int_{-\infty}^{\infty} \epsilon(n, n', t - t') \delta \ddot{\gamma}_{n'}(t') dt' = f_n(t) \end{aligned} \quad (\text{B6})$$

with

$$f_n(t) = \begin{cases} \bar{\omega}_p^2 \delta \gamma_j(t) - \omega_p^2 \sin(\theta_j + \omega t) & n = j \in I \\ 0 & \text{else.} \end{cases} \quad (\text{B7})$$

Writing

$$f_j(t) = f_j e^{-i\omega t} + c.c. \quad (\text{B8})$$

the amplitude of the driving term for a resistive junction is given by

$$f_j = \bar{\omega}_p^2 \delta \gamma_j - i \frac{\omega_p^2}{2} e^{-i\theta_j}. \quad (\text{B9})$$

Introducing the spatial Fourier transform (n goes over all junctions)

$$\gamma(q_z) = \frac{1}{N_z} \sum_n \delta \gamma_n e^{-iq_z z_n} \quad (\text{B10})$$

we obtain

$$\begin{aligned} \gamma(q_z) &= G(q_z, \omega) \sum_{j \in I} f_j e^{-iq_z z_j} \\ &= G(q_z, \omega) \sum_{j \in I} \left[\bar{\omega}_p^2 \delta \gamma_j - i \frac{\omega_p^2}{2} e^{-i\theta_j} \right] e^{-iq_z z_j} \end{aligned} \quad (\text{B11})$$

with the Green's function of the homogeneous equation

$$G^{-1}(q_z, \omega) = \bar{\omega}_p^2 - i\omega \frac{\sigma}{\epsilon_0} - \omega^2 \epsilon_{\text{ph}}^L(q_z, \omega). \quad (\text{B12})$$

From this an equation for $\delta \gamma_i$ in the resistive junctions is obtained:

$$\sum_{j \in I} (G^{-1}(i, j, \omega) - \bar{\omega}_p^2 \delta_{i,j}) \delta \gamma_j = -i \frac{\omega_p^2}{2} e^{-i\theta_i} \quad (\text{B13})$$

with

$$G(i, j, \omega) = \frac{1}{N_z} \sum_q G(q, \omega) e^{iq(z_i - z_j)}. \quad (\text{B14})$$

Using

$$\bar{\epsilon}_{\text{ph}}(i, k, \omega) = -\frac{1}{\omega^2} G^{-1}(i, k, \omega) + \left(\frac{\bar{\omega}_p^2}{\omega^2} - \frac{i\sigma}{\epsilon_0 \omega} \right) \delta_{i,k} \quad (\text{B15})$$

we get

$$\delta \gamma_i = i \frac{\omega_p^2}{2\omega^2} \sum_{k \in I} \left[\bar{\epsilon}_{\text{ph}}(i, k, \omega) + \frac{i\sigma}{\epsilon_0 \omega} \delta_{i,k} \right]^{-1} e^{-i\theta_k}, \quad (\text{B16})$$

which gives us the dc-component Eq. (B5) of the current density

$$\begin{aligned} j(V) &= \sigma E_{dc} \\ &- j_c \frac{\omega_p^2}{2\omega^2} \text{Im} \sum_{k \in I} e^{i\theta_k} \left[\bar{\epsilon}_{\text{ph}}(i, k, \omega) + \frac{i\sigma}{\epsilon_0 \omega} \delta_{i,k} \right]^{-1} e^{-i\theta_k}. \end{aligned} \quad (\text{B17})$$

Finally we want to note that the dielectric function $\bar{\epsilon}_{\text{ph}}(i, k, \omega)$ can also be used to write the RSJ equations in a form where only the phases $\gamma_i(t)$, of the resistive junctions $i \in I$ enter:

$$\begin{aligned} j &= j_c \sin \gamma_i(t) + \sigma \frac{\hbar}{2ed} \dot{\gamma}_i(t) \\ &+ \frac{\epsilon_0 \hbar}{2ed} \sum_{j \in I} \int_{-\infty}^{\infty} \bar{\epsilon}_{\text{ph}}(i, j, t - t') \ddot{\gamma}_j(t') dt'. \end{aligned} \quad (\text{B18})$$

¹ R. Kleiner, F. Steinmeyer, G. Kunkel, P. Müller, Phys. Rev. Lett. **68**, 2394 (1992).
² R. Kleiner, P. Müller, Phys. Rev. B **49** (1994), 1327.
³ K. Schlenga, G. Hechtfischer, R. Kleiner, W. Walkenhorst, P. Müller, Phys. Rev. Lett. **76**, 4943 (1996).
⁴ A. Yurgens, D. Winkler, N. Zavaritsky, T. Claeson, Proceedings of SPIE, Vol **2697**, 433 (1996).
⁵ P. Seidel, A. Pfuch, U. Hübner, F. Schmidl, H. Schneidewind, T. Ecke, J. Scherbel, Physica C **293**, 49 (1997).
⁶ Ch. Helm, Ch. Preis, F. Forsthofer, J. Keller, K. Schlenga, R. Kleiner, P. Müller, Phys. Rev. Lett. **79**, 737 (1997).
⁷ Ch. Helm, Ch. Preis, F. Forsthofer, J. Keller, K. Schlenga, R. Kleiner, P. Müller, Physica C **293**, 60 (1997).
⁸ K. Schlenga, R. Kleiner, G. Hechtfischer, M. Möble, S. Schmitt, P. Müller, Ch. Helm, Ch. Preis, F. Forsthofer, J. Keller, H. L. Johnson, M. Veith, E. Steinbeiß, Phys. Rev. B **57**, 14518 (1998).
⁹ T. Zetterer, M. Franz, J. Schützmann, W. Ose, H.H. Otto, K.F. Renk, Phys. Rev. B 41, 9499 (1990); V.M. Burlakov, S.V. Shulga, J. Keller, K.F. Renk, Physica C **203**, 68 (1992) and references therein.
¹⁰ R.G. Buckley, M.P. Staines, D.M. Poole, T. Stoto, N.E. Flower, Physica C **248**, 247 (1995) and references therein.
¹¹ A. A. Tsvetkov, D. Dulić, D. van der Marel, A. Damascelli, G. A. Kaljushnaia, J. I. Gorina, N. N. Senturina, B. Willemse, N. N. Kolesnikov, Z. F. Ren, J. H. Wang, A. A. Menovsky, T. T. M. Palstra, preprint.
¹² P. Berberich, R. Buemann, H. Kinder, Phys. Rev. Lett. **49**, 1500 (1982).
¹³ Ya.G. Ponomarev, E.B. Tsokur, M.V. Sudakova, S.N. Tchernoskov, M.A. Lorenz, M.A. Hein, G. Müller, H. Piel, B.A. Animov, preprint.
¹⁴ T. Koyama, M. Tachiki, Phys. Rev. B **54**, 16183 (1996).
¹⁵ Ch. Preis, Ch. Helm, J. Keller, A. Sergeev, R. Kleiner, SPIE Conference Proceedings “Superconducting Superlattices II: Native and Artificial”, Vol **3480**, 236 (1998).

¹⁶ Ch. Preis et al, to be published.

¹⁷ E.G. Maksimov, P.I. Arseev, N.S. Maslova, preprint cond-mat 9812422.

¹⁸ R. Zeyher, G. Zwicknagl, Solid State Commun. **66**, 617 (1988); R. Zeyher, G. Zwicknagl, Z. Phys. B- Condensed Matter **78**, 175 (1990).

¹⁹ A. Yurgens, private communication.

²⁰ S. Tajima, G. D. Gu, S. Miyamoto, A. Odagawa, N. Koshizuka, Phys. Rev. B **48**, 16164 (1993).

²¹ C.-S. Jia, P.-Y. Lin, Y. Xiao, X.-W. Jiang, X.-Y. Gou, S. Huo, H. Li, Q.-B. Yang, Physica C **268**, 41 (1996).

²² A. D. Kulkarni, J. Prade, F. W. de Wette, W. Kress, U. Schröder, Phys. Rev. B **40**, 2642 (1989).

²³ A. D. Kulkarni, F. W. de Wette, J. Prade, U. Schröder, W. Kress, Phys. Rev. B **43**, 5451 (1991).

²⁴ J. Prade, A. D. Kulkarni, F. W. de Wette, U. Schröder, W. Kress, Phys. Rev. B **39**, 2771 (1989).